

Direct photons in Pb+Pb at CERN-SPS from microscopic transport theory

A. Dumitru, M. Bleicher, S.A. Bass, C. Spieles, L. Neise, H. Stöcker, W. Greiner

Institut für Theoretische Physik der J.W. Goethe-Universität

Postfach 111932, D-60054 Frankfurt a.M., Germany

(August 22, 2018)

Direct photon production in central Pb+Pb collisions at CERN-SPS energy is calculated within the relativistic microscopic transport model UrQMD, and within distinctly different versions of relativistic hydrodynamics. We find that in UrQMD the local momentum distributions of the secondaries are strongly elongated along the beam axis initially. Therefore, the pre-equilibrium contribution dominates the photon spectrum at transverse momenta above ≈ 1.5 GeV. The hydrodynamics prediction of a strong correlation between the temperature and radial expansion velocities on the one hand and the slope of the transverse momentum distribution of direct photons on the other hand thus is not recovered in UrQMD. The rapidity distribution of direct photons in UrQMD reveals that the initial conditions for the longitudinal expansion of the photon source (the meson “fluid”) resemble rather boostinvariance than Landau-like flow.

The radiation of real and virtual photons has frequently been proposed as a diagnostic tool for the hot and dense matter created in (ultra-) relativistic heavy-ion collisions [1,2]. The mean free path of photons with high transverse momentum exceeds the expected source sizes by one order of magnitude [2,3]. Hard photons thus can give insight into the early stage of these reactions.

Transverse momentum dependent upper limits for direct photon production in central S+Au collisions at 200A GeV have been published by the WA80 collaboration [4]. These data initiated theoretical studies [5–8] which showed that direct photon production is strongly overestimated if the photon source is thermalized (having an initial energy density of 2 – 5 GeV/fm³) and if one assumes that it is composed of light mesons only (say π , η , ρ , ω). Due to the low specific entropy of these particles a reasonable final-state multiplicity of secondaries and a maximum temperature that is consistent with the WA80 data ($T_{max} \leq 300$ MeV) can not be achieved simultaneously (at least if the expansion is approximately isentropic).

Most of the calculations quoted (except those of ref. [6]), however, assumed that the photon source is in local thermal equilibrium and that ideal hydrodynamics can be applied to determine the space-time evolution of the temperature. Here, we perform a calculation within the microscopic transport model UrQMD, which includes the pre-equilibrium contributions to direct photon production. This is of particular relevance in view of the fact that local thermalization (i.e. locally isotropic momentum distributions) in (ultra-) relativistic heavy-ion collisions is probably not achieved within the first few fm/c [9,10] where the high- k_T photons are produced. Since neither thermal nor chemical equilibrium is assumed, the effects of finite viscosity (i.e. finite mean free paths) [11] and inhomogeneous or fluctuating energy density distributions [12] are included. Comparisons of the transverse momentum and rapidity distributions of direct photons with those calculated within various fluid-dynamical models are made.

The calculations presented here are based on the UrQMD model [13], which spans the

entire presently available range of energies from SIS to SPS. It's collision term contains 50 different baryon species (including nucleon, delta and hyperon resonances with masses up to 2.2 GeV) and 25 different meson species (including strange meson resonances), which are supplemented by their corresponding antiparticles and all isospin-projected states.

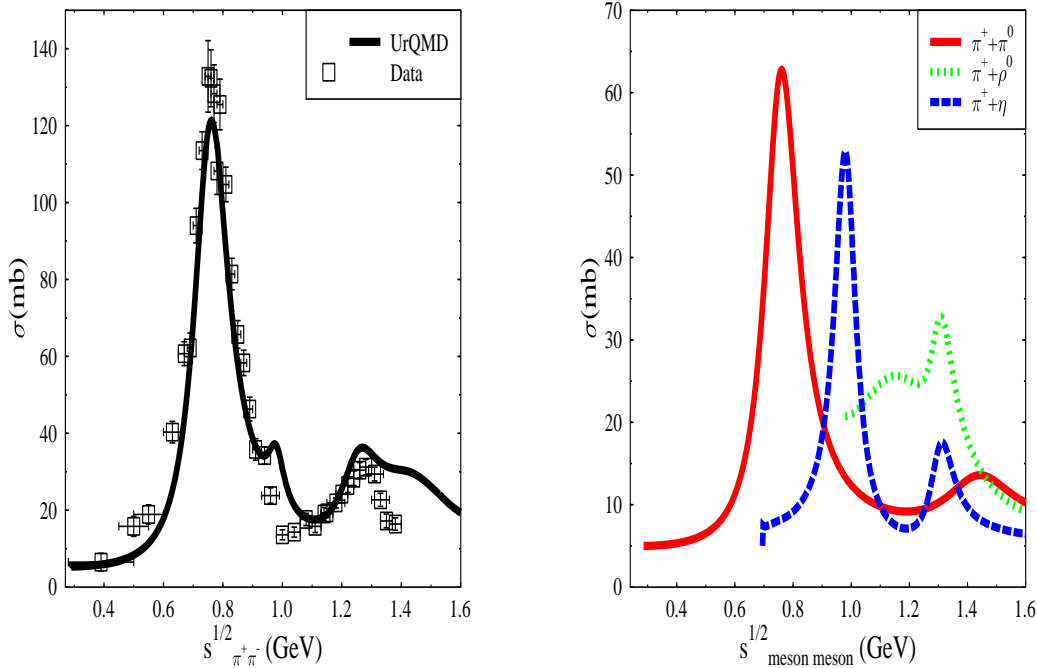


FIG. 1. Total cross sections of $\pi^+\pi^-$ and various other meson-meson reactions as calculated within the UrQMD model, data from ref. [14].

The model is based on the covariant propagation of all hadrons on classical trajectories, excitation of resonances and strings and their subsequent decay resp. fragmentation. UrQMD accounts for secondary interactions: the annihilation of produced mesons on baryons can lead to the formation of s -channel resonances or strings. Free cross-sections for hadron-hadron scattering in the hot and dense nuclear matter are employed. Comparisons of UrQMD calculations to experimental hadron yields from SIS to SPS are documented elsewhere [13].

We briefly discuss the two most important reactions for the creation of direct photons. Below 2 GeV center of mass energy intermediate resonance states are excited. The total cross section for these reactions are given by

$$\sigma_{\text{tot}}^{M_1 M_2}(\sqrt{s}) = \sum_{R=\rho, f_2, \dots} \langle j_{M_1}, m_{M_1}, j_{M_2}, m_{M_2} || J_R, M_R \rangle \frac{2I_R + 1}{(2I_{M_1} + 1)(2I_{M_2} + 1)} \times \frac{\pi}{p_{CM}^2} \frac{\Gamma_{R \rightarrow M_1 M_2} \Gamma_{\text{tot}}}{(M_R - \sqrt{s})^2 + \frac{\Gamma_{\text{tot}}^2}{4}}, \quad (1)$$

which depends on the total decay width Γ_{tot} , the partial decay width $\Gamma_{R \rightarrow M_1 M_2}$ and on the c.m. energy \sqrt{s} . At higher energies these processes become less important. One then enters the region of t-channel scattering of the hadrons.

UrQMD predicts a rich and non-trivial resonance structure in the meson-meson scattering cross section. In fig. 1 (left) the total $\pi^+ \pi^-$ cross section as calculated within UrQMD is compared to experimental data [14]. Below 1 GeV the spectrum is dominated by the ρ resonance, while at higher energy the $f_2(1270)$ gets important.

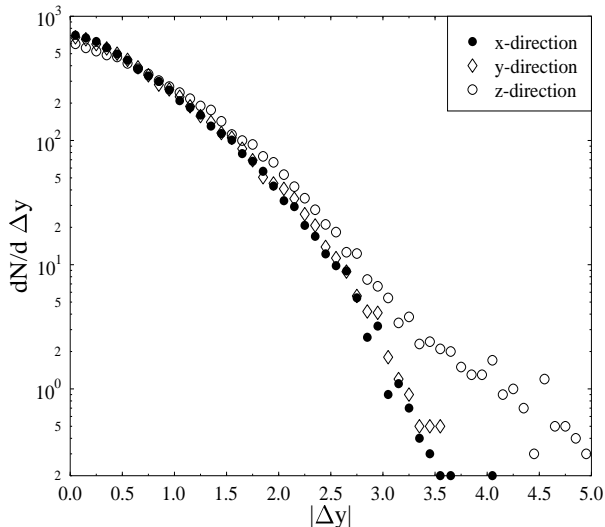


FIG. 2. Number of $\pi\pi$ collisions as a function of the rapidity difference in the three spacial directions (Pb+Pb, $E_{Lab} = 160A$ GeV, $b = 0$ fm).

Figure 2 shows the distribution of $\pi\pi$ collisions with a given relative rapidity in a given

spacial direction (upper indices refer to the particle number):

$$\Delta y_{x,y,z} = \frac{1}{2} \ln \frac{E^1 + p_{x,y,z}^1}{E^1 - p_{x,y,z}^1} - \frac{1}{2} \ln \frac{E^2 + p_{x,y,z}^2}{E^2 - p_{x,y,z}^2} . \quad (2)$$

One observes that most collisions occur at $|\Delta y| < 3$. In this range the collision-spectrum is nearly isotropic, corresponding to a temperature of $T = 180 \pm 30$ MeV. In the longitudinal direction, however, there is an additional component above $|\Delta y_z| = 3$. This is due to pions created in the fragmentation of a color flux tube close to projectile and target rapidities. In p(200A GeV)+p collisions $\approx 15\%$ of all pions have $|y_{CM}^\pi| > 2$ [15]. Note that not all of these collisions are forbidden by the finite formation time of secondaries since the fragmentation region mesons contain one of the initial valence quarks (i.e. the sources of the color field). Thus, even within the formation time, these mesons may interact with half of the free meson cross section in the UrQMD model. Obviously, these meson-meson collisions with large longitudinal rapidity difference are not taken into account in hydrodynamical calculations. However, as will be discussed below, it is just their contribution which dominates the direct photon spectrum above $k_T \approx 1.5$ GeV.

Let us now get to the reference equilibrium calculations of direct photon production within hydrodynamics. Here we assume either a three-dimensional expansion with cylindrical symmetry and longitudinal boost invariance [16] or a one-dimensional expansion with Landau initial conditions (i.e. $v = 0$ at time $t = 0$). In both cases the dynamical creation of the fluid of secondaries in space-time is ignored and only the expansion stage is treated.

In the three-fluid model fluids one and two correspond to projectile and target, while fluid three represents the newly produced particles around midrapidity. Fluids one and two are coupled via source terms leading to energy and momentum exchange. These interactions are due to binary collisions of the nucleons in the respective fluids and are derived from nucleon-nucleon data. A detailed discussion of this model as well as results (pion rapidity and transverse momentum spectra at CERN-SPS, baryon stopping and directed flow at AGS and SPS, the width of the compression shock waves etc.) can be found in refs. [8,17,18].

In the hydrodynamical calculations the fluid of produced particles is assumed to be the hottest, and thus the dominant source of high- k_T photons. Its equation of state is that of an ideal gas of massive π , η , ρ , and ω mesons below $T_C = 160$ MeV. For $T > T_C$ we assume an ideal QGP (massless, noninteracting u , d quarks and gluons) described within the MIT bag-model [19]. The bag constant is chosen such that the pressures of the two phases match at $T = T_C$ ($B^{1/4} = 235$ MeV) thus leading to a first order phase transition.

The number of emitted direct photons in each of the three phases is parametrized as [2]

$$E \frac{dN^\gamma}{d^4x d^3k} = \frac{5\alpha\alpha_S}{18\pi^2} T^2 e^{-E/T} \ln \left(\frac{2.912E}{g^2 T} + 1 \right) . \quad (3)$$

E is the photon energy in the local rest frame. In our calculations we fix $\alpha_S = g^2/4\pi = 0.4$. Eq. (3) accounts for pion annihilation ($\pi\pi \rightarrow \rho\gamma$), and Compton-like scattering ($\pi\rho \rightarrow \pi\gamma$, $\pi\eta \rightarrow \pi\gamma$) off a ρ or η meson (in lowest order perturbation theory). In the QGP phase, alternatively, quark-antiquark annihilation ($q\bar{q} \rightarrow g\gamma$) and Compton-like scattering of a quark or antiquark off a gluon ($q, \bar{q} + g \rightarrow q, \bar{q} + \gamma$) are considered. Contributions from the A_1 meson [20], as well as the effect of hadronic formfactors [2], are neglected since they are of the same magnitude as higher order corrections to eq. (3), which we have also not taken into account. Also, the number of processes that contribute to direct photon production enhances the rate only linearly, while the temperature distribution enters exponentially. Our main interest here is not the absolute photon yield but rather the effective temperature of the direct photons, i.e. the inverse slope of their transverse momentum spectrum.

The photon spectrum emitted in a heavy-ion collision is obtained here by an (incoherent) integration over space-time:

$$\frac{dN^\gamma}{d^2k_T dy} = \int d^4x E \frac{dN^\gamma}{d^4x d^3k} . \quad (4)$$

To allow for a comparison with the hydrodynamical calculations we have considered the same processes also in the UrQMD model, namely $\pi^\pm\pi^\mp \rightarrow \rho^0\gamma$, $\pi^\pm\pi^0 \rightarrow \rho^\pm\gamma$, $\pi^\pm\rho^0 \rightarrow \pi^\pm\gamma$, $\pi^\pm\rho^\mp \rightarrow \pi^0\gamma$, $\pi^0\rho^\pm \rightarrow \pi^\pm\gamma$, $\pi^\pm\eta \rightarrow \pi^\pm\gamma$. Of course, in UrQMD these processes are considered

explicitly (we employ the differential cross sections given in ref. [2]) and are not folded with thermal distribution functions, nor with a thermal \sqrt{s} -distribution of meson-meson collisions. We find that the $\pi\rho \rightarrow \pi\gamma$ and $\omega \rightarrow \pi\gamma$ processes are dominant in the range $1 \text{ GeV} \leq k_T \leq 3 \text{ GeV}$. This is due to the fact that, in addition to the kinetic energy, also the mass of the ρ or ω can be converted into photon energy. In contrast to the thermal rate (3), in the UrQMD model m_ρ and m_ω are smeared out according to a Breit-Wigner distribution. For the processes $\pi\pi \rightarrow \rho\gamma$ we have, however, assumed that the ρ -meson in the final state is produced with the peak mass of 770 MeV. Since free current-quarks and gluons have not been included in the present version of the UrQMD model, the processes $q\bar{q} \rightarrow g\gamma$ etc. are not considered there.

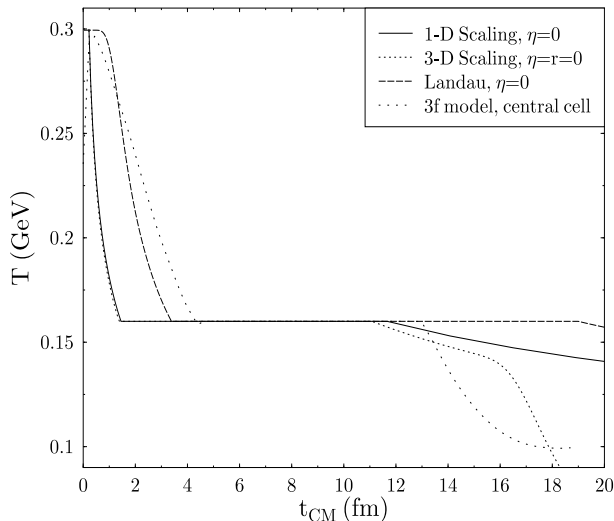


FIG. 3. Temperature in the central region as a function of time in various hydrodynamical models, Pb+Pb-collisions ($b = 0 \text{ fm}$) at CERN-SPS.

The temperature of the newly produced particles in the central region is depicted in fig. 3 [17]. In case of a Bjorken expansion we have assumed an initial temperature of 300 MeV and an initial time of $\tau_0 = 0.22 \text{ fm}/c$, while for the Landau expansion we take an initial longitudinal extension of $2L = 2R_{\text{Pb}}/\gamma_{CM} \approx 1.4 \text{ fm}$. The maximum temperature in the

three-fluid model is determined by the coupling terms between fluids one and two (and, of course, by the equation of state of fluid three). The produced particles cool most swiftly in scaling hydrodynamics, while in the case of a Landau expansion the temperature at midrapidity is constant until the rarefaction waves reach the center. In this latter case one finds the longest-living mixed phase. This is due to the fact that we assumed purely one-dimensional (longitudinal) expansion.

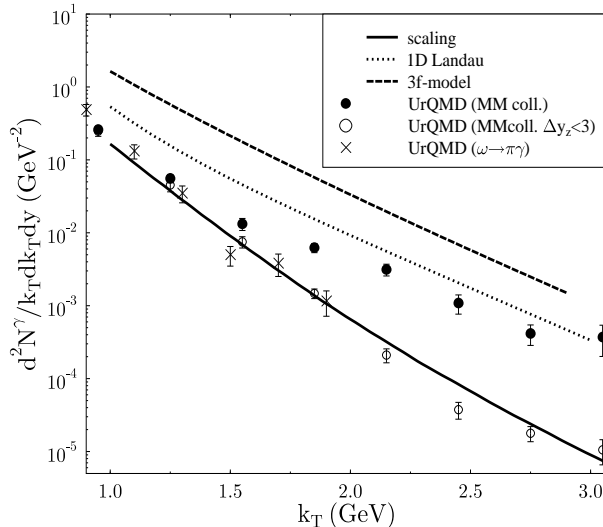


FIG. 4. Transverse momentum spectrum of direct photons at midrapidity (Pb+Pb, $E_{Lab} = 160A$ GeV, $b = 0$ fm). The lines refer to hydrodynamical calculations including a first order phase transition to a QGP at $T_C = 160$ MeV (three-fluid model (dashed), scaling expansion (solid), and Landau expansion (dotted)). The result of the UrQMD calculation with all meson-meson collisions (full circles) is compared to the calculation with only “thermal” meson-meson collisions (open circles). Crosses show the photons from ω -meson decays, which are as many as those from “thermal” meson-meson collisions. Above $k_T \approx 1.5$ GeV the pre-equilibrium contribution dominates.

The various transverse momentum distributions of direct photons, cf. fig. 4, reflect the distinct cooling laws. The faster the cooling of the photon source, the steeper the slope of the photon spectrum. An exponential fit of the spectrum in the region $2 \text{ GeV} \leq k_T \leq 3 \text{ GeV}$

yields “ T ” = 260 MeV both for the three-fluid model and for the Landau expansion, and “ T ” = 210 MeV for the Bjorken expansion.

If we take into account only the “thermal” meson-meson collisions with rapidity gap $|\Delta y_z| < 3$, we find a similar photon spectrum in the UrQMD model as in scaling hydrodynamics. The fact that the hadronic mass spectrum in UrQMD has no upper limit leads to a collision spectrum of the light mesons that is equally “cool” as in the hydrodynamic calculations, if there a first order phase transition at a critical temperature around 160 MeV is assumed (cf. also ref. [7]). In UrQMD, a significant part of the energy density can be stored into heavy meson- and baryon resonances. This keeps the pressure and temperature low [9,21]. We have analyzed the temperature as a function of energy density (at normal nuclear matter baryon density) in UrQMD in ref. [13].

One also observes that the “pre-equilibrium” meson-meson collisions with $|\Delta y_z| > 3$ dominate the emission of direct photons with large transverse momenta, $k_T > 1.5$ GeV. Obviously, this contribution has nothing to do with high meson transverse momenta (“temperatures”) or fast collective radial expansion. It is thus not included in the hydrodynamic calculations. Hence, the strong correlation between the (Doppler-shifted) temperature and the slope of the photon transverse momentum distribution predicted by the hydrodynamical calculations (see also refs. [5,7,8,22]) is not seen in UrQMD. Meson-baryon and baryon-baryon processes may further enhance the pre-equilibrium contribution [23]. Below $k_T = 1.5$ the photons are dominantly produced by “thermal” meson-meson collisions and $\omega \rightarrow \pi\gamma$ decays.

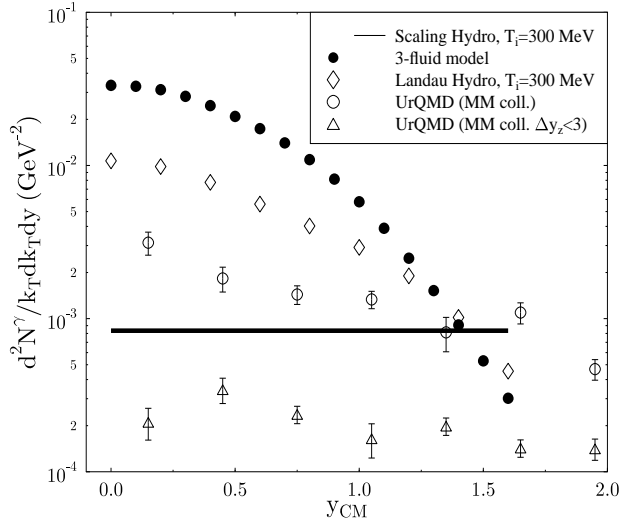


FIG. 5. Rapidity distribution of direct photons, calculated within the various hydrodynamical models (for $k_T = 2$ GeV) and UrQMD (for $k_T = 2.15$ GeV).

The rapidity distribution of the secondaries (or, alternatively, of the temperature) at early times is very different in the various hydrodynamical models [17,24]. While $T(\eta)$ (η denotes the fluid rapidity) is strongly peaked around midrapidity in the three-fluid and Landau models, scaling flow $v_z = z/t$ and energy-momentum conservation, $\partial_\mu T^{\mu\nu} = 0$, imply that the pressure $p(T, \mu_B)$ is independent of the fluid rapidity, $\partial_\eta p = 0$, and depends only on proper time, $\tau = \sqrt{t^2 - z^2}$. For net baryon-free matter $\partial_\eta T = 0$ follows. However, even in the first case matter is accelerated by a (longitudinal) rarefaction wave, leading to a broadening of the rapidity distribution. Thus, in any case, at the late freeze-out stage the rapidity distribution of secondaries (around midrapidity) will be more or less flat. On the other hand, the rapidity distribution of direct photons with transverse momenta much larger than the maximum temperature of the photon source (e.g. $k_T \approx 2$ GeV at SPS) offers the opportunity to measure the rapidity distribution of the hot photon source *at early times* [24]. This is demonstrated in fig. 5. In the three-fluid model and in the Landau-

expansion the photon rapidity distribution is strongly peaked around midrapidity. It is not proportional to the (squared) rapidity distribution of the pions, which are emitted at the much later freeze-out stage. The distribution obtained within UrQMD only resembles that for a boostinvariant expansion, if only “thermal” meson-meson collisions are taken into account. The full calculation predicts a maximum of the photon- dN/dy at midrapidity. This is so because the photon spectrum emitted in elementary meson-meson reactions with large Δy is peaked around midrapidity. Nevertheless, the photon distribution is considerably flatter than in the three-fluid or Landau models, which show a concave curvature in this logarithmic plot. This is a consequence of the longitudinal velocity profile [25] induced by the (longitudinal) rarefaction wave accelerating the fluid that is initially at rest. The UrQMD calculation does not exhibit this characteristic feature.

In summary, we have calculated direct photon production in central Pb+Pb collisions at CERN-SPS energy within a microscopic transport model (UrQMD). Within this model, secondary hadron production is described by color flux tube fragmentation and resonance decay. This leads to non-thermal momentum distributions, i.e. they are strongly elongated along the beam axis initially. The contribution from this pre-equilibrium stage to direct photon production is found to dominate at transverse momenta above ≈ 1.5 GeV. Thus, within the UrQMD model, the slope of the photon transverse momentum spectrum is not directly related to the Doppler-shifted “transverse temperature” of the source, as it is in hydrodynamics.

If only “thermal” meson-meson collisions are taken into account, both the transverse momentum and rapidity spectra of direct photons in UrQMD resemble those calculated within boostinvariant hydrodynamics, if for the latter one assumes an initial temperature $T_i = 300$ MeV and initial time $\tau_i = 0.22$ fm. This is so although QGP formation is not assumed in UrQMD. Hence, heavy resonances and color flux tubes allow for a rather soft meson-meson collision spectrum even at high entropies.

ACKNOWLEDGMENTS

This work was supported by Graduiertenkolleg Theoretische und Experimentelle Schwerionophysik, BMBF, DFG, and GSI. M. Bleicher thanks the Josef Buchmann foundation for financial support.

[1] see e.g.

E.V. Shuryak: *Phys. Lett.* **B78**, 150 (1978);

B. Sinha: *Phys. Lett.* **B128**, 91 (1983);

L. McLerran, T. Toimela: *Phys. Rev. D* **31**, 545 (1985);

P.V. Ruuskanen: *Nucl. Phys.* **A544**, 169c (1992);

J. Kapusta: *Nucl. Phys.* **A566**, 45c (1994);

B. Müller: *Rept. Prog. Phys.* **58**, 611 (1995);

J.W. Harris, B. Müller: *Ann. Rev. Nucl. Part. Sci.* **46**, 71 (1996)

[2] J. Kapusta, P. Lichard, D. Seibert: *Phys. Rev. D* **44**, 2774 (1991)

[3] M.H. Thoma: *Phys. Rev. D* **51**, 862 (1995)

[4] R. Albrecht et al.: *Phys. Rev. Lett.* **76**, 3506 (1996)

[5] D.K. Srivastava, B. Sinha: *Phys. Rev. Lett.* **73**, 2421 (1994);

N. Arbex, U. Ornik, M. Plümer, A. Timmermann, R.M. Weiner: *Phys. Lett.* **B345**, 307 (1995);

J.J. Neumann, D. Seibert, G. Fai: *Phys. Rev. C* **51**, 1460 (1995);

Y. Tarsov: *Phys. Lett.* **B379**, 279 (1996);

C.M. Hung, E.V. Shuryak: *Phys. Rev. C* **56**, 453 (1997)

[6] E.L. Bratkovskaya, W. Cassing: *Nucl. Phys.* **A619**, 413 (1997);

G.Q. Li, G.E. Brown, C.M. Ko: nucl-th/9706022;

- G.Q. Li, G.E. Brown: nucl-th/9706076
- [7] J. Sollfrank, P. Huovinen, M. Kataja, P.V. Ruuskanen, M. Prakash, R. Venugopalan: *Phys. Rev. C* **55**, 392 (1997);
J. Cleymans, K. Redlich, D.K. Srivastava: *Phys. Rev. C* **55**, 1431 (1997)
- [8] A. Dumitru, U. Katscher, J.A. Maruhn, H. Stöcker, W. Greiner, D.H. Rischke: *Phys. Rev. C* **51**, 2166 (1995)
- [9] H. Sorge: *Phys. Lett.* **B402**, 251 (1997)
- [10] R. Mattiello, C. Hartnack, A.v. Keitz, J. Schaffner, H. Sorge, H. Stöcker, C. Greiner: *Nucl. Phys. B (Proc. Suppl.)* **24B**, 221 (1991)
- [11] P. Danielewicz: *Phys. Lett.* **B146**, 168 (1984);
P. Danielewicz, M. Gyulassy: *Phys. Rev. D* **31**, 53 (1985);
A. Hosoya, K. Kajantie: *Nucl. Phys.* **B250**, 666 (1985);
K. Haglin, S. Pratt: *Phys. Lett.* **B328**, 255 (1994)
- [12] C. Spieles, L. Gerland, H. Stöcker, C. Greiner, C. Kuhn, J.P. Coffin: *Phys. Rev. Lett.* **76**, 1776 (1996);
M. Gyulassy, D.H. Rischke, B. Zhang: *Nucl. Phys.* **A613**, 397 (1997)
- [13] M. Bleicher et al.: *Proc. of the Int. Conf. on Nuclear Physics at the Turn of the Millenium*, “Structure of Vacuum and Elementary Matter”, Wilderness/George (South Africa), March 10–16, 1996, World Scientific, Singapore, 1997, p. 452;
S. Bass et al.: *ibid.* p. 399
- [14] S.D. Protopopescu et al.: *Phys. Rev. D* **7**, 1279 (1973)
- [15] T. Kafka et al.: *Phys. Rev. D* **16**, 1261 (1977)
- [16] K. Kajantie, L. McLerran: *Phys. Lett.* **B119**, 203 (1982); *Nucl. Phys.* **B214**, 261 (1983);

- J.D. Bjorken: *Phys. Rev. D* **27**, 140 (1983);
- K. Kajantie, R. Raitio, P.V. Ruuskanen: *Nucl. Phys.* **B222**, 152 (1983);
- H. von Gersdorff, M. Kataja, L. McLerran, P.V. Ruuskanen: *Phys. Rev. D* **34**, 794 (1986)
- [17] A. Dumitru, J. Brachmann, M. Bleicher, J.A. Maruhn, H. Stöcker, W. Greiner: *Heavy Ion Phys.* **5**, 357 (1997)
- [18] J. Brachmann, A. Dumitru, J.A. Maruhn, H. Stöcker, W. Greiner, D.H. Rischke: *Nucl. Phys.* **A619**, 391 (1997)
- [19] A. Chodos, R.L. Jaffe, K. Johnson, C.B. Thorn, V.F. Weisskopf: *Phys. Rev. D* **9**, 3471 (1974);
 S.A. Chin: *Phys. Lett.* **B78**, 552 (1978);
 E.V. Shuryak: *Phys. Rep.* **61**, 71 (1980);
 J. Cleymans, R.V. Gavai, E. Suhonen: *Phys. Rep.* **130**, 217 (1986);
 H. Stöcker, W. Greiner: *Phys. Rep.* **137**, 277 (1986)
- [20] L. Xiong, E. Shuryak, G.E. Brown: *Phys. Rev. D* **46**, 3798 (1992);
 C. Song: *Phys. Rev. C* **47**, 2861 (1993)
- [21] H. Stöcker, W. Greiner, W. Scheid: *Z. Phys.* **A286**, 121 (1978);
 H. Stöcker, A.A. Ogloblin, W. Greiner: *Z. Phys.* **A303**, 259 (1981);
 H. Bebie, P. Gerber, J.L. Goity, H. Leutwyler: *Nucl. Phys.* **B378**, 95 (1992)
- [22] D. Seibert: *Z. Phys.* **C58**, 307 (1993)
- [23] C. Spieles, L. Gerland, N. Hammon, M. Bleicher, S.A. Bass, H. Stöcker, W. Greiner: hep-ph/9706525 (submitted to *Z. Phys. C*)
- [24] A. Dumitru, U. Katscher, J.A. Maruhn, H. Stöcker, W. Greiner, D.H. Rischke: *Z. Phys.* **A353**, 187 (1995)
- [25] D.H. Rischke, S. Bernard, J.A. Maruhn: *Nucl. Phys.* **A595**, 346 (1995)